

Wavelet Based Homogenization of a 2 Dimensional Elliptic Problem.

Y. Capdeboscq and M.S. Vogelius*

February 24, 2004

Abstract

In this paper we derive explicit approximate averaging formulas for the second order coefficients of a two dimensional periodic elliptic operator using non overlapping wavelets, and we present the algorithm used to derive such formulas. We compare the averaged operators obtained to the ones given by the theory of homogenization, in the cases where explicit formulas are known. Finally we present numerical experiments to document the effectiveness of this explicit homogenization approach for coefficients that are far from periodic.

1 Introduction

The development of numerical methods designed to capture the global behavior of solutions of partial differential equations without resolving the fine scale details has been the subject of many investigations; such numerical schemes are generally referred to as numerical homogenization methods. In this paper, we follow the theory of homogenization approach, that is, to average the coefficients of the equation so that the solution of the problem solved with these (smoothed) coefficients is close to the solution of the original problem on a coarse scale. An advantage of such a strategy is that it is unrelated to the numerical scheme used to solve the homogenized (or averaged) problem. Furthermore, the averaging formulas we derive are explicit and local, i.e., practically free in terms of computational cost. Based on specific physical considerations, various heuristic algebraic averaging formulas have been derived (see [18] for a review of such methods); to our knowledge, a systematic and consistent method to derive averaging formulas was not available.

We should mention that numerical homogenization is not restricted to coefficient averaging strategies. In the context of wavelet or multigrid based numerical homogenization [3, 8, 10, 11, 13] the partial differential operator can be reduced to its coarse scale effect. Alternatively, adapted finite elements can be developed to capture the small scale effects [14], or the resolution of the small scale can be localized [4]. In both cases, the goal is to reduce the computational cost of a numerical resolution method for a given problem. In contrast, focusing solely on the coefficients allows to choose numerical resolution methods independently of the treatment of the coefficients. However, we were able to derive such formulas in a special case of periodic coefficient; the method we propose to use such coefficients in a non periodical medium is a numerical experiment.

The use of the built-in multiscale structure of wavelet representations to homogenize (correctly average) rough coefficients of elliptic boundary value problems was initiated by Beylkin and Brewster

*Department of Mathematics, Rutgers University, New Brunswick, NJ 08903, USA

[8], and has since been the subject of several investigations. In this multiresolution context, homogenization consists in the sequential projection (reduction) of the elliptic operators onto coarser and coarser, adjacent scales. This approach can be applied to any elliptic operator without particular assumptions on the behavior of the coefficients with respect to the fine and coarse scales. However, to rigorously relate solutions obtained from this numerical procedure to analytic results from homogenization theory it is often convenient to consider the case of periodic fine scale variations. Comparisons with results from the theory of homogenization have been established in the one dimensional case by Dorobantu and Engquist [10], and by Gilbert [12], but in two (and higher) dimensions very little is known concerning the asymptotic effectiveness of such numerical “wavelet homogenization procedures”. Dorobantu and Engquist have proved that, starting from a (two dimensional) discrete operator

$$L_{J+1} = \frac{1}{h^2} \left(\Delta_+^x A^{(1,1)} \Delta_-^x + \Delta_+^x A^{(1,2)} \Delta_-^y + \Delta_+^y A^{(2,1)} \Delta_-^x + \Delta_+^y A^{(2,2)} \Delta_-^y \right) ,$$

where Δ_+ and Δ_- are the forward and backward undivided difference operators, the coarse-scale solutions obtained by “Haar homogenization” may (asymptotically) be viewed as solutions for a similar operator of divergence form. However, Dorobantu and Engquist provide no specific information about the coefficients of this “effective” operator. For higher order wavelets, similar “invariance results” have been established by Beylkin and Coult [7] for certain classes of pseudo-differential operators (see also Beylkin, Coifman and Rokhlin [6]).

The basic step of the multiscale reduction procedure involves the computation of a Schur complement (by Gaussian elimination). The matrix corresponding to the fine scale finite difference discretization has a band structure. In the case of Haar wavelets the above result of Dorobantu and Engquist shows that the matrix that emerges after elimination of “wavelet” variables (reduction to the coarser scale) is itself well approximated by a band diagonal matrix corresponding to a finite difference approximation of a divergence form operator.

The aim of this paper is to examine the explicit (asymptotic) form of the coefficients one obtains using specific such multiscale reduction procedures, and to compare these to recently established exact homogenization formulas for 2×2 isotropic periodic arrays.

To be precise we follow the approach initiated by Dorobantu and Engquist, which essentially relies on “maximal periodicity” of the coefficients and on the non overlapping support of the basis functions at a fixed scale. The non overlapping support leads to fairly simple recurrence relations for the passing between two adjacent scales that may be solved explicitly; the “maximal periodicity” ensures that the homogenization is accomplished in one step. Starting with a discrete operator of the form

$$L_{J+1} = \frac{1}{h^2} \left(\Delta_+^x A^1 \Delta_-^x + \Delta_+^y A^2 \Delta_-^y \right) , \quad (1.1)$$

with $h = 2^{-(J+1)}$, we suppose that the coefficients $A^1(x, y)$ and $A^2(x, y)$ are piecewise constant, each constant attained on a “pixel” of size $h \times h$. The periodicity assumption is that the functions $A^1(x, y)$ and $A^2(x, y)$ are periodic with period $2h$. In other words, the function $A^i(x, y)$ is defined

by (infinite) periodic extension of the $2h \times 2h$ stencil

$$\begin{array}{|c|c|}
 \hline
 A_{2k,2l+1}^i & A_{2k+1,2l+1}^i \\
 \hline
 A_{2k,2l}^i & A_{2k+1,2l}^i \\
 \hline
 \end{array} \tag{1.2}$$

In this framework we show that the reduced operator corresponding to the coarse-scale variables (those on scale $2h$) asymptotically approaches

$$L_H = \frac{1}{(2h)^2} \left(\Delta_+^x H^{(1,1)} \Delta_-^x + \Delta_+^x H^{(1,2)} \Delta_-^y + \Delta_+^y H^{(2,1)} \Delta_-^x + \Delta_+^y H^{(2,2)} \Delta_-^y \right) ,$$

where the coefficient matrix H is *constant*. But most important for analytic comparisons, our calculations lead to an explicit formula for H . We initially perform our calculations for Haar wavelet representations, however, subsequently we describe the results of a similar calculation for the next level of so called multiwavelet representations (as introduced in [2]).

When the starting operator (1.1) is isotropic, that is when $A^1(x, y) = A^2(x, y)$, the effective (continuously homogenized) operator corresponding to a four phase periodic array has recently been determined explicitly, [9]. We compare the Haar based wavelet homogenization formula and the multiwavelet homogenization formula to this continuous homogenization formula. As one would expect, the wavelet homogenization procedure does not always asymptotically agree with the continuous formula – the wavelet based formulas, however, are quite interesting and do provide the basis for very direct “averaging methods” that may be applied in cases where continuous formulas are not known, if one desires an approach which is faster than a full multiscale reduction procedure.

Somewhat to our surprise the wavelet homogenization procedures do (asymptotically) for a locally isotropic, periodic array lead to the “continuous” formula for the determinant of the homogenized matrix. In the locally anisotropic case, where a “continuous” formula is not yet known, the two multiscale reduction procedures produce identical determinants, (4.9), which may give a strong indication of what the “continuous” result should be. For the trace, however, we do in general only obtain a rough approximation.

At the very end of this paper we provide some numerical experiments to document the effectiveness of the (explicit) wavelet homogenization formulas when applied to patterns that are far from periodic.

2 Decomposition of the discrete, Haar based difference operator

We briefly review the decomposition of the discrete operator L_{J+1} which forms the basis for the analysis of Dorobantu and Engquist. The starting discrete operator has the form

$$L_{J+1} = \frac{1}{h^2} (\Delta_+^x A^1 \Delta_-^x + \Delta_+^y A^2 \Delta_-^y) ,$$

where the backward difference operators Δ_-^y , and Δ_-^x are defined by

$$\Delta_-^y (u)_{n,p} = (u_{n,p} - u_{n,p-1}) , \quad \text{and} \quad \Delta_-^x (u)_{n,p} = (u_{n,p} - u_{n-1,p}) ,$$

respectively. Multiplication by A^i is performed componentwise, i.e.

$$A^i (u)_{n,p} = (A_{n,p}^i u_{n,p}) ,$$

and the forward difference operators Δ_+^y , and Δ_+^x are defined by

$$\Delta_+^y (u)_{n,p} = (u_{n,p+1} - u_{n,p}) , \quad \text{and} \quad \Delta_+^x (u)_{n,p} = (u_{n+1,p} - u_{n,p}) ,$$

respectively. In fact, L_{J+1} is the natural 5-points discrete approximation to the elliptic operator $\nabla \cdot (A \nabla \cdot)$. The arguments for these operators are two dimensional arrays $(u_{n,p})_{n,p \in \mathcal{Z}}$. Just as in the case of the coefficients, A^i , we also identify the arrays $(u_{n,p})$ with piecewise constant functions on a rectangular grid of mesh size $h = 2^{-J-1}$

$$u(x, y) = \sum_{n,m} u_{n,m} \phi_{J+1,n}(x) \phi_{J+1,m}(y) .$$

Here $\phi_{J+1,n} = \phi(2^{J+1}x - n)$, and ϕ is the indicator function of the segment $[0, 1]$. In other words, the coefficients $u_{n,m} 2^{-(J+1)}$ are a representation of u on the scale $J+1$. The initial discretization space is

$$V_{J+1} = V_{J+1}^x \otimes V_{J+1}^y \quad \text{with} \quad V_J^t = \text{span}\{\phi_{J,k}(t), k \in \mathfrak{J}_t\} .$$

The set of indices \mathfrak{J}_t being such that we stay within the square domain considered. For either of the two variables (i.e., $t = x$ or $t = y$) we have

$$V_{J+1}^t = V_J^t \oplus W_J^t ,$$

where W_J^t is spanned by the wavelet functions $\psi_{J,k}(t) = \psi(2^J t - k)$, with the mother wavelet ψ given by

$$\psi(t) = \begin{cases} 1 & \text{if } 0 \leq t \leq \frac{1}{2}, \\ -1 & \text{if } \frac{1}{2} \leq t \leq 1, \\ 0 & \text{otherwise} . \end{cases}$$

We have the following orthogonal decomposition

$$\begin{aligned} V_{J+1} &= (W_J^x \otimes W_J^y) \oplus (W_J^x \otimes V_J^y) \oplus (V_J^x \otimes W_J^y) \oplus (V_J^x \otimes V_J^y) \\ &= (W_J^x \otimes W_J^y) \oplus (W_J^x \otimes V_J^y) \oplus (V_J^x \otimes W_J^y) \oplus V_J . \end{aligned}$$

In order to represent the operator L_{J+1} in accordance with this decomposition, we must calculate the representations for the operators Δ_{\pm}^x , Δ_{\pm}^y and multiplication by A^i using this orthogonal decomposition. It can be observed that the difference operators “naturally respect” the \otimes operation, in

the sense that $\Delta_{\pm}^x = \Delta_{\pm} \otimes I_d$, and $\Delta_{\pm}^y = I_d \otimes \Delta_{\pm}$. Therefore the calculations become essentially one dimensional and give, see [10],

$$\frac{1}{h} \Delta_{\pm}^y \leftrightarrow \frac{1}{2h} \begin{array}{cccc|c} \mp 4I_d - \Delta_{\pm}^y & \mp \Delta_{\pm}^y & 0 & 0 & W \otimes W \\ \pm \Delta_{\pm}^y & \Delta_{\pm}^y & 0 & 0 & W \otimes V \\ 0 & 0 & \mp 4I_d - \Delta_{\pm}^y & \mp \Delta_{\pm}^y & V \otimes W \\ 0 & 0 & \pm \Delta_{\pm}^y & \Delta_{\pm}^y & V \otimes V \\ \hline & W \otimes W & W \otimes V & V \otimes W & V \otimes V \end{array}$$

$$\frac{1}{h} \Delta_{\pm}^x \leftrightarrow \frac{1}{2h} \begin{array}{cccc|c} \mp 4I_d - \Delta_{\pm}^x & 0 & \mp \Delta_{\pm}^x & 0 & W \otimes W \\ 0 & \mp 4I_d - \Delta_{\pm}^x & 0 & \mp \Delta_{\pm}^x & W \otimes V \\ \pm \Delta_{\pm}^x & 0 & \Delta_{\pm}^x & 0 & V \otimes W \\ 0 & \pm \Delta_{\pm}^x & 0 & \Delta_{\pm}^x & V \otimes V \\ \hline & W \otimes W & W \otimes V & V \otimes W & V \otimes V \end{array}$$

Here we have dropped the sub- and superscripts from the spaces V and W , using the convention that the first element in a direct products always refer to the x variable. A simple calculation also gives that multiplication by A^i is represented by the matrix

$$\begin{bmatrix} a_1^i & a_2^i & a_3^i & a_4^i \\ a_2^i & a_1^i & a_4^i & a_3^i \\ a_3^i & a_4^i & a_1^i & a_2^i \\ a_4^i & a_3^i & a_2^i & a_1^i \end{bmatrix}$$

with

$$\begin{aligned} a_1^i(k, l) &= \begin{bmatrix} + & + \\ + & + \end{bmatrix} = \frac{1}{4} (A_{2k, 2l}^i + A_{2k+1, 2l}^i + A_{2k, 2l+1}^i + A_{2k+1, 2l+1}^i), \\ a_2^i(k, l) &= \begin{bmatrix} - & - \\ + & + \end{bmatrix} = \frac{1}{4} (A_{2k, 2l}^i + A_{2k+1, 2l}^i - A_{2k, 2l+1}^i - A_{2k+1, 2l+1}^i), \\ a_3^i(k, l) &= \begin{bmatrix} + & - \\ + & - \end{bmatrix} = \frac{1}{4} (A_{2k, 2l}^i - A_{2k+1, 2l}^i + A_{2k, 2l+1}^i - A_{2k+1, 2l+1}^i), \\ a_4^i(k, l) &= \begin{bmatrix} - & + \\ + & - \end{bmatrix} = \frac{1}{4} (A_{2k, 2l}^i - A_{2k+1, 2l}^i - A_{2k, 2l+1}^i + A_{2k+1, 2l+1}^i), \end{aligned}$$

We note that due to the periodicity of $A^1(x, y)$ and $A^2(x, y)$ the constants a_1^i, a_2^i, a_3^i and a_4^i are independent of k and l , *i.e.*, $a_j^i = a_j^i I_d \otimes I_d$, $i = 1, 2, j = 1, \dots, 4$. The computation of the decomposition for the operator L_{J+1} now simply consists of matrix multiplications.

3 The one dimensional case

Let us first recall what happens in the one dimensional case. The decomposed operator is

$$\frac{2}{(2h)^2} \begin{bmatrix} L_1 & -(a_1 + a_2)\Delta_+\Delta_- - 2(a_1 + a_2)\Delta_- \\ -(a_1 + a_2)\Delta_+\Delta_- + 2(a_1 + a_2)\Delta_+ & (a_1 + a_2)\Delta_+\Delta_- \end{bmatrix}$$

where

$$L_1 = -8I_d a_1 - (a_1 + a_2)\Delta_+\Delta_- ,$$

and where $a_1 = \frac{1}{2}(A_{2k} + A_{2k+1})$ and $a_2 = \frac{1}{2}(A_{2k} - A_{2k+1})$. After a one step Gaussian elimination, we obtain

$$\begin{bmatrix} \frac{2}{(2h)^2}L_1 & -\frac{2}{(2h)^2}((a_1 + a_2)\Delta_+\Delta_- + 2(a_1 + a_2)\Delta_-) \\ 0 & \bar{L}_J \end{bmatrix} .$$

The reduced (coarse scale) operator is given by

$$\bar{L}_J = \frac{1}{(2h)^2}\Delta_+H\Delta_- , \quad (3.1)$$

with

$$H = 2(a_1 + a_2)I_d - 2(a_1 + a_2)^2(\Delta_- - 2I_d)L_1^{-1}(\Delta_+ + 2I_d) .$$

In order to obtain an explicit asymptotic approximation to \bar{L}_J , one observes that L_1^{-1} can be expressed in the form of a convergent Neumann series. To see this we write

$$\begin{aligned} L_1 &= -(6a_1 - 2a_2)I_d - (a_1 + a_2)(S_1 + S_{-1}) \\ &= -(6a_1 - 2a_2)\left(I_d - q\frac{(S_1 + S_{-1})}{2}\right), \quad q = -\frac{a_1 + a_2}{3a_1 - a_2} , \end{aligned}$$

where $(S_{\pm 1}(u))_n = u_{n\pm 1}$ are the standard shift operators. Ellipticity implies that $|a_2| < |a_1|$, and $|q| < 1$, and since $\|S_1 + S_{-1}\|_\infty \leq 2$ it now follows that L_1^{-1} may be expressed as a convergent Neumann series. Alternatively, we can write

$$L_1 = -8a_1\left(I_d + q_2\frac{\Delta_+\Delta_-}{4}\right) , \quad (3.2)$$

with $0 < q_2 = \frac{a_1 + a_2}{2a_1} < 1$. Since $\|\Delta_+\Delta_-\|_\infty = \|S_1 + S_{-1} - 2I_d\|_\infty \leq 4$, the decomposition (3.2) also leads to a convergent Neumann series for L_1^{-1} . For convenience we shall use the latter series even though $|q| < q_2$ (and the former therefore is more rapidly convergent). We calculate

$$\begin{aligned} H &= 2(a_1 + a_2)I_d - \frac{(a_1 + a_2)^2}{a_1}I_d + R\Delta_+\Delta_- , \quad (3.3) \\ \text{with } R &= \frac{(a_1 + a_2)^2}{4a_1}\left(-1 + \sum_{k=0}^{\infty}(-1)^{k+1}\frac{q_2^{k+1}}{4^{k+1}}(\Delta_+\Delta_-)^k(\Delta_- - 2I_d)(\Delta_+ + 2I_d)\right) . \end{aligned}$$

The lowest order term in H thus becomes $\alpha I_d = \frac{a_1^2 - a_2^2}{a_1}I_d = \frac{2A_{2k}A_{2k+1}}{A_{2k} + A_{2k+1}}I_d$, *i. e.*, multiplication with the harmonic average of the fine scale coefficients, as predicted by homogenization theory. Introduction of the expression (3.3) for H into (3.1) now yields

$$\bar{L}_J = \frac{\alpha}{(2h)^2}\Delta_+\Delta_- + \frac{1}{(2h)^2}R(\Delta_+\Delta_-)^2 .$$

R is a bounded operator in the maximum norm, and therefore we may conclude that

$$\left\|\bar{L}_J v - \frac{\alpha}{(2h)^2}\Delta_+\Delta_- v\right\|_\infty \leq h^2 C \|v^{(4)}\|_\infty . \quad (3.4)$$

Using the first expansion, in terms of elementary shift operators, Dorobantu and Engquist proved with a more sophisticated proof that the constant C can in fact be bounded by $\frac{K}{(\log(q))^2}$, with K a universal constant, independent of the A 's. In the two dimensional case, many more coefficients are

involved, and the complexity of their structure (presented in the appendix) makes a precise study of the constants involved very difficult, and probably not even that useful.

It is quite relevant to point out that in order to show that the coarse scale reduced operator is asymptotically equivalent to $\frac{\alpha}{(2h)^2}\Delta_+\Delta_-$ (as was done by the estimate (3.4)) it is not necessary to insist that $|q_2| < 1$ in the formula for L_1 . Suppose L_1 was given by

$$L_1 = c_0 I_d + c_1 \Delta_+ \Delta_- + h^4 R \quad ,$$

where c_0 and c_1 are constants (independent of h), satisfying $0 < |c_0|, |c_1| < \infty$, and where R stands for any operator satisfying $\|R(v)\|_\infty \leq C \|v^{(k)}\|_\infty$, for some $k \geq 0$ and C independent of h . We define $\Delta^n = (S_1)^n + (S_1^{-1})^n - 2I_d$ and note that $\Delta^1 = \Delta_+ \Delta_-$. A Taylor expansion yields $\Delta^n = n^2 \Delta^1 + h^4 R$, (since $\Delta^n f(x) = n^2 f^{(2)}(x) + \frac{n^4}{4!} f^{(4)}(\xi)$) so that $L_1 = L_1^* + h^4 R = c_0 (I_d + \frac{c_1}{n^2 c_0} \Delta^n) + h^4 R$. Since $\|\Delta^n\|_\infty = 4$ for all n , it suffices to select $n > 2\sqrt{\frac{c_1}{c_0}}$ in order for the first term (L_1^*) to be invertible in terms of a convergent Neumann series. For such n we conclude that

$$(L_1^*)^{-1} L_1 = I_d + h^4 R \quad , \quad (3.5)$$

with $(L_1^*)^{-1} = \frac{1}{c_0} I_d + h^2 R$. The operator resulting from a one step ‘‘approximate’’ Gaussian elimination, using $(L_1^*)^{-1}$ in place of L_1^{-1} , becomes

$$\begin{bmatrix} \frac{2}{(2h)^2} L_1 & -\frac{2}{(2h)^2} ((a_1 + a_2) \Delta_+ \Delta_- + 2(a_1 + a_2) \Delta_-) \\ h^3 R & \bar{L}_J \end{bmatrix} \quad ,$$

with

$$\bar{L}_J = \frac{1}{(2h)^2} \Delta_+ H \Delta_- \quad ,$$

$$H = (a_1 + a_2) - (a_1 + a_2)^2 (\Delta_- - 2I_d) (L_1^*)^{-1} (\Delta_+ + 2I_d) = \alpha I_d + h^2 R \quad .$$

We thus have an estimate like (3.4), and for sufficiently smooth solutions this again shows that the limiting coarse scale reduced operator amounts to $\frac{\alpha}{(2h)^2} \Delta_+ \Delta_-$. We shall use the ‘‘trick’’ just described extensively in our two dimensional calculations; in that case we shall actually need two terms of the approximate inverse, that is we shall need the equivalent of

$$(L_1^*)^{-1} = \frac{1}{c_0} I_d - \frac{c_1}{n^2 (c_0)^2} \Delta^n + h^4 R = \frac{1}{c_0} I_d - \frac{c_1}{(c_0)^2} \Delta_+ \Delta_- + h^4 R \quad . \quad (3.6)$$

Indeed, in two dimensions we shall do most of our calculations modulo operators of order h^4 . The identities (3.5) and (3.6) simply express the fact that modulo operators of order h^4 the operator L_1 has an inverse which is given by the first two terms of its formal Neumann series.

4 Derivation of the 2d homogenized operator

The operator L_{j+1} is (up to a scaling of $\frac{1}{4h^2}$) represented by

$$\begin{bmatrix} -16a_1^2 I_d - 2(a_1^1 + a_2^2) \Delta_{yy} & -2(a_1^2 + a_2^2) D_y & -16a_3^2 I_d - 2(a_3^2 + a_4^2) \Delta_{yy} & -2(a_3^2 + a_4^2) D_y \\ -16a_1^1 I_d - 2(a_1^1 + a_3^1) \Delta_{xx} & -16a_2^1 I_d - 2(a_2^1 + a_4^1) \Delta_{xx} & -2(a_1^1 + a_3^1) D_x & -2(a_2^1 + a_4^1) D_x \\ 2(a_1^2 + a_2^2) D_y & 2(a_1^2 + a_2^2) \Delta_{yy} & 2(a_4^2 + a_3^2) D_y & 2(a_4^2 + a_3^2) \Delta_{yy} \\ -16a_2^2 I_d - 2(a_2^2 + a_4^2) \Delta_{xx} & -16a_1^1 I_d - 2(a_1^1 + a_3^1) \Delta_{xx} & -2(a_2^2 + a_4^2) D_x & -2(a_1^1 + a_3^1) D_x \\ -16a_3^2 I_d - 2(a_3^2 + a_4^2) \Delta_{yy} & -2(a_3^2 + a_4^2) D_y & -16a_1^1 I_d - 2(a_1^1 + a_2^2) \Delta_{yy} & -2(a_1^2 + a_2^2) D_y \\ +2(a_3^1 + a_4^1) D_x & +2(a_2^1 + a_4^1) D_x & +2(a_3^1 + a_4^1) \Delta_{xx} & +2(a_2^1 + a_4^1) \Delta_{xx} \\ 2(a_4^2 + a_3^2) D_y & 2(a_4^2 + a_3^2) \Delta_{yy} & 2(a_1^2 + a_2^2) D_y & 2(a_1^2 + a_2^2) \Delta_{yy} \\ +2(a_2^2 + a_4^2) D_x & +2(a_3^2 + a_4^2) D_x & +2(a_2^2 + a_4^2) \Delta_{xx} & +2(a_3^2 + a_4^2) \Delta_{xx} \end{bmatrix}$$

Here D_x and D_y denote the centered difference operators $D_x = \Delta_+^x + \Delta_-^x = S_x - S_x^{-1}$ and $D_y = S_y - S_y^{-1}$. Furthermore $\Delta_{xx} = \Delta_+^x \Delta_-^x$ and $\Delta_{yy} = \Delta_+^y \Delta_-^y$. In the sequel, we shall also use the notation Δ_{xy} for $\frac{1}{4} D_x D_y (= \frac{1}{2} \Delta_+^x \Delta_-^y + \frac{1}{2} \Delta_-^x \Delta_+^y)$ up to fourth order.

In order to obtain the reduced coarse scale operator, we must perform 3 eliminations. Except for the first, these eliminations are all performed modulo operators of order h^4 , relying on the remarks made at the end of the previous section. The fairly extensive algebraic calculations are performed by means of Maple; we provide a summary of the results of these calculations, but for more information about the details we refer to “<http://www.math.rutgers.edu/~yrcr/WaveHom/>”. We shall denote by $L_{nn}^{(n)}$ the diagonal term after the (n-1)st step. The reduced coarse scale (the wavelet homogenized) operator is therefore asymptotically $\bar{L}_J = \frac{1}{(2h)^2} L_{44}^{(4)}$.

First inversion, $L_{11}^{(1)}$.

The top left diagonal operator is given by

$$L_{11}^{(1)} = -16(a_1^1 + a_1^2) I_d - 2(a_1^1 + a_3^1) \Delta_{xx} - 2(a_1^2 + a_2^2) \Delta_{yy} .$$

Since L_{j+1} is elliptic, $|a_2^1|, |a_3^1|, |a_4^1| < a_1^1$, and $|a_2^2|, |a_3^2|, |a_4^2| < a_1^2$. Therefore $L_{11}^{(1)}$ may be written in the form

$$L_{11}^{(1)} = -16(a_1^1 + a_1^2) (I_d + B_1)$$

where $B_1 = \frac{1}{8(a_1^1 + a_1^2)} ((a_1^1 + a_3^1) \Delta_{xx} + (a_1^2 + a_2^2) \Delta_{yy})$ is a bounded linear operator, with

$$\|B_1\|_\infty \leq \frac{|a_1^1 + a_3^1|}{8(a_1^1 + a_1^2)} \|\Delta_{xx}\|_\infty + \frac{|a_1^2 + a_2^2|}{8(a_1^1 + a_1^2)} \|\Delta_{yy}\|_\infty \leq \frac{1}{2} + \frac{|a_3^1| + |a_2^2|}{2(a_1^1 + a_1^2)} < 1.$$

Consequently, the Neumann expansion for $(L_{11}^{(1)})^{-1}$ is convergent, and we can write

$$(L_{11}^{(1)})^{-1} = -\frac{1}{16(a_1^1 + a_1^2)} I_d + \frac{1}{128(a_1^1 + a_1^2)^2} ((a_1^1 + a_3^1) \Delta_{xx} + (a_1^2 + a_2^2) \Delta_{yy}) - \frac{1}{16(a_1^1 + a_1^2)} B_1^2 \sum_{k=0}^{\infty} (-B_1)^k .$$

B_1^2 is a fourth order difference operator: $\|B_1^2 v\|_\infty < Ch^4 \|v^{(4)}\|_\infty$, where C depends on a_1^1, a_1^2, a_2^2 and a_3^1 , but is independent of h . In other words

$$(L_{11}^{(1)})^{-1} = -\frac{1}{16(a_1^1 + a_1^2)} I_d + \frac{1}{128(a_1^1 + a_1^2)^2} ((a_1^1 + a_3^1) \Delta_{xx} + (a_1^2 + a_2^2) \Delta_{yy}) + h^4 R . \quad (4.1)$$

Here, and in sequel, R denotes a linear operator which is bounded independently of h (when acting on sufficiently smooth functions).

Second inversion, $L_{22}^{(2)}$.

After one (column) elimination we obtain , using the fact that $D_y D_y = 4\Delta_{yy} + h^4 R$,

$$\begin{aligned} L_{22}^{(2)} &= -16a_1^1 I_d - 256 (a_2^1)^2 (L_{11}^{(1)})^{-1} \\ &\quad + 2 \left(a_2^2 + a_1^2 + 8 \left(2a_2^2 a_1^2 + (a_2^2)^2 + (a_1^2)^2 \right) (L_{11}^{(1)})^{-1} \right) \Delta_{yy} \\ &\quad - 2 \left(a_3^1 + a_1^1 + 32 \left(a_2^1 a_4^1 + (a_2^1)^2 \right) (L_{11}^{(1)})^{-1} \right) \Delta_{xx} + h^4 R . \end{aligned} \quad (4.2)$$

Insertion of (4.1) into (4.2) now gives

$$L_{22}^{(2)} = c_{0,2} I_d + c_{1,2} \Delta_{xx} + c_{2,2} \Delta_{yy} + h^4 R , \quad (4.3)$$

with

$$c_{0,2} = -16 \frac{a_1^1 a_1^2 + (a_1^1)^2 - (a_2^1)^2}{a_1^1 + a_1^2} < 0 ,$$

thanks to the ellipticity of L_{J+1} . The coefficients $c_{1,2}$ and $c_{2,2}$ are given in the appendix. Supposing $A^1 = A^2$, upper bounds for $|c_{1,2}|$ and $|c_{2,2}|$ are $6a_1^1 (= 6a_1^2)$ and $4a_1^1 (= 4a_1^2)$, respectively. A lower bound for $|c_{0,2}|$ is $8a_1^1 = 8a_1^2$. These bounds are not sufficient to insure convergence of the natural Neumann series corresponding to $L_{22}^{(2)}$. They lead only to a bound for the norm of $\frac{c_{1,2}}{c_{0,2}} \Delta_{xx} + \frac{c_{2,2}}{c_{0,2}} \Delta_{yy}$ of the size $\frac{6 \cdot 4 + 4 \cdot 4}{8} = 5 > 1$ (when $a_1^1 = a_1^2$). This is a conservative estimate: a numerically better, but still not sufficient bound, $\frac{5}{2}$, can be established. A decomposition into elementary shift operators does not seem to provide a bound lower than one either. We shall therefore proceed along the lines outlined at the end of Section 3. Given $n > 0$, Let Δ_{xx}^n be defined by $\Delta_{xx}^n = S_x^n + S_x^{-n} - 2I_d$. By a Taylor expansion one obtains that $\Delta_{xx} = \frac{1}{n^2} \Delta_{xx}^n + h^4 R$. Substituting $\frac{1}{n^2} \Delta_{xx}^n$ and the similar operator $\frac{1}{n^2} \Delta_{yy}^n$ into (4.3) we obtain

$$L_{22}^{(2)} = L_{22}^{(2)*} + h^4 R = c_{0,2} (I_d + B_2) + h^4 R ,$$

where

$$B_2 = \frac{c_{1,2}}{n^2 c_{0,2}} \Delta_{xx}^n + \frac{c_{2,2}}{n^2 c_{0,2}} \Delta_{yy}^n$$

satisfies $\|B_2\|_\infty < \frac{4}{n^2} \left(\frac{|c_{1,2}| + |c_{2,2}|}{|c_{0,2}|} \right)$. The Neumann series for $(L_{22}^{(2)*})^{-1}$ is now convergent if we choose $n > 2 \sqrt{\frac{|c_{1,2}| + |c_{2,2}|}{|c_{0,2}|}}$ (a finite such n always exist $|c_{0,2}| > 0$), and furthermore

$$\left(L_{22}^{(2)*} \right)^{-1} = \frac{1}{c_{0,2}} \left(I_d - \frac{c_{1,2}}{n^2 c_{0,2}} \Delta_{xx}^n - \frac{c_{2,2}}{n^2 c_{0,2}} \Delta_{yy}^n \right) + h^4 R = \frac{1}{c_{0,2}} \left(I_d - \frac{c_{1,2}}{c_{0,2}} \Delta_{xx} - \frac{c_{2,2}}{c_{0,2}} \Delta_{yy} \right) + h^4 R . \quad (4.4)$$

We may use this operator in place of an exact inverse of $L_{22}^{(2)}$ to eliminate below diagonal elements of the second column, modulo operators of order h^4 . Unlike in the one dimensional case we need the exact form of the second term of $\left(L_{22}^{(2)*} \right)^{-1}$ (the term of order h^2) since the off-diagonal entries contain elements of order 1 (and the final operator $L_{44}^{(4)}$ is of order h^2).

Third inversion, $L_{33}^{(3)}$.

After the second (column) elimination, modulo terms of order h^4 , we have

$$L_{33}^{(3)} = c_{0,3} I_d + c_{1,3} \Delta_{xx} + c_{2,3} \Delta_{yy} + c_{3,3} \Delta_{xy} + h^4 R,$$

with constants $c_{1,3}$, $c_{2,3}$ and $c_{3,3}$ as given in the appendix, and

$$c_{0,3} = -16 \frac{a_1^1 \left((a_1^2)^2 - (a_3^2)^2 \right) + a_1^2 \left((a_1^1)^2 - (a_2^1)^2 \right)}{a_1^1 a_1^2 + (a_1^1)^2 - (a_2^1)^2} < 0 .$$

Numerical examples show that the ratio $\frac{|c_{1,3}|+|c_{2,3}|+|c_{3,3}|}{|c_{0,3}|}$ is not uniformly bounded by 1/4 as needed to argue for convergence of the Neumann series. In the spirit of the previous inversion, we introduce the operator Δ_{xy}^n , defined in terms of S_x^n, S_y^n, S_x^{-n} and S_x^{-n}

$$\Delta_{xy}^n = \frac{1}{4} (S_x^n - S_x^{-n})(S_y^n - S_y^{-n}) ,$$

and we verify that $\Delta_{xy}^n = n^2 \Delta_{xy} + h^4 R$. Expressed in terms of these operators

$$L_{33}^{(3)} = c_{0,3} \left(I_d + \frac{c_{1,3}}{c_{0,3} n^2} \Delta_{xx}^n + \frac{c_{2,3}}{c_{0,3} n^2} \Delta_{yy}^n + \frac{c_{3,3}}{c_{0,3} n^2} \Delta_{xy}^n \right) + h^4 R = L_{33}^{(3)*} + h^4 R .$$

Choosing $n > 2\sqrt{\frac{|c_{1,3}|+|c_{2,3}|+|c_{3,3}|}{|c_{0,3}|}}$ (a finite such n exist since we established that $|c_{0,3}| > 0$) we obtain a convergent Neumann series for $(L_{33}^{(3)*})^{-1}$, and thus

$$\begin{aligned} (L_{33}^{(3)*})^{-1} &= \frac{1}{c_{0,3}} \left(I_d - \frac{c_{1,3}}{c_{0,3} n^2} \Delta_{xx}^n - \frac{c_{2,3}}{c_{0,3} n^2} \Delta_{yy}^n - \frac{c_{3,3}}{c_{0,3} n^2} \Delta_{xy}^n \right) + h^4 R \\ &= \frac{1}{c_{0,3}} \left(I_d - \frac{c_{1,3}}{c_{0,3}} \Delta_{xx} - \frac{c_{2,3}}{c_{0,3}} \Delta_{yy} - \frac{c_{3,3}}{c_{0,3}} \Delta_{xy} \right) + h^4 R . \end{aligned} \quad (4.5)$$

We then proceed to eliminate elements below the diagonal in the third column, modulo terms of order h^4 .

The discrete, homogenized operator, $L_{44}^{(4)}$.

After the third (column) elimination we arrive at the coarse scale reduced (homogenized) operator. Modulo fourth order terms (and a scaling factor $\frac{1}{4h^2}$) it reads $L_{44}^{(4)} = H_{11} \Delta_{xx} + 2H_{12} \Delta_{xy} + H_{22} \Delta_{yy} + h^4 R$, where the matrix H is given by

$$H = \begin{bmatrix} X_1 & 0 \\ 0 & Y_2 \end{bmatrix} - \frac{1}{X_2 + Y_1} \begin{bmatrix} (Z_1)^2 & Z_1 Z_2 \\ Z_1 Z_2 & (Z_2)^2 \end{bmatrix} \quad (4.6)$$

and where the constants $X_i, Y_i, Z_i, i = 1, 2$, are defined by

$$\begin{aligned} X_i &= \frac{(a_1^i)^2 - (a_3^i)^2}{a_1^i} = \frac{1}{\frac{1}{A_{2k,2l}^i + A_{2k,2l+1}^i} + \frac{1}{A_{2k+1,2l}^i + A_{2k+1,2l+1}^i}} , \\ Y_i &= \frac{(a_1^i)^2 - (a_2^i)^2}{a_1^i} = \frac{1}{\frac{1}{A_{2k,2l}^i + A_{2k+1,2l}^i} + \frac{1}{A_{2k,2l+1}^i + A_{2k+1,2l+1}^i}} , \\ Z_i &= \frac{a_1^i a_4^i - a_2^i a_3^i}{a_1^i} = \frac{A_{2k,2l}^i A_{2k+1,2l+1}^i - A_{2k+1,2l}^i A_{2k,2l+1}^i}{A_{2k,2l}^i + A_{2k+1,2l}^i + A_{2k,2l+1}^i + A_{2k+1,2l+1}^i} . \end{aligned}$$

The coefficient $X_i = h_x(m_y(A^i))$ is the harmonic average in the x-axis direction of the arithmetic averages in the y-axis direction (of A^i). The coefficient $Y_i = h_y(m_x(A^i))$ is the opposite: the harmonic average in the y-axis direction of the arithmetic averages in the x-axis direction (of A^i).

The coefficient Z_i is the (normalized) determinant of fine grid coefficients (of A^i). The eigenvalues of the matrix H are given by

$$\lambda_1 = \frac{X_1 + Y_2}{2} - \frac{(Z_1)^2 + (Z_2)^2}{2(X_2 + Y_1)} + \sqrt{\left(\frac{X_1 - Y_2}{2} - \frac{(Z_1)^2 - (Z_2)^2}{2(X_2 + Y_1)}\right)^2 + \frac{(Z_1 Z_2)^2}{(X_2 + Y_1)^2}} \quad (4.7)$$

$$\lambda_2 = \frac{X_1 + Y_2}{2} - \frac{(Z_1)^2 + (Z_2)^2}{2(X_2 + Y_1)} - \sqrt{\left(\frac{X_1 - Y_2}{2} - \frac{(Z_1)^2 - (Z_2)^2}{2(X_2 + Y_1)}\right)^2 + \frac{(Z_1 Z_2)^2}{(X_2 + Y_1)^2}} \quad (4.8)$$

The determinant of H may be expressed as

$$\det(H) = \frac{X_1 Y_2}{X_2 + Y_1} (\tilde{X}_2 + \tilde{Y}_1) \quad , \quad (4.9)$$

where

$$\tilde{X}_i = m_y(h_x(A^i)) \quad \text{and} \quad \tilde{Y}_i = m_x(h_y(A^i)) \quad .$$

We note that the \tilde{X}_i, \tilde{Y}_i and the X_i, Y_i, Z_i are related by the formulas

$$\tilde{X}_i = X_i - \frac{(Z_i)^2}{Y_i} \quad \text{and} \quad \tilde{Y}_i = Y_i - \frac{(Z_i)^2}{X_i} \quad .$$

The trace of H is

$$\text{trace}(H) = X_1 \frac{X_2 + \tilde{Y}_1}{X_2 + Y_1} + Y_2 \frac{\tilde{X}_2 + Y_1}{X_2 + Y_1} \quad . \quad (4.10)$$

Incidentally, the formulas for the determinant and the trace immediately imply that H is a positive definite, symmetric matrix. For the locally isotropic case ($A^1 = A^2$) it is not hard to verify that H is bounded from below by the harmonic average of the components and from above by the arithmetic average.

5 Comparison to continuous homogenization formulas

The continuous analogue of the operator (1.1) is $\mathfrak{L}_h = \nabla \cdot (A(x/h, y/h) \nabla)$, where the matrix valued function $A(x, y)$ is given by

$$A(x, y) = \begin{bmatrix} A^1(x, y) & 0 \\ 0 & A^2(x, y) \end{bmatrix} \quad ,$$

and the functions $A^i(x, y)$ are defined by infinite periodic extensions of the arrays shown in (1.2). It is well known that there exists a symmetric positive definite matrix $\mathfrak{A} = \text{Hom}(A)$ with associated operator $\mathfrak{L} = \nabla \cdot (\mathfrak{A} \nabla)$, such that $(\mathfrak{L}_h)^{-1} \rightarrow (\mathfrak{L})^{-1}$ as $h \rightarrow 0$ (under appropriate boundary conditions) see [5]. The operator \mathfrak{L} and the matrix \mathfrak{A} are referred to as the ‘‘continuously’’ homogenized operator and homogenized matrix associated to A , respectively. For the 2×2 periodic arrays studied here a variety of information is available concerning exact formulas for the homogenized matrix. Starting from the diagonal matrix valued function $A(x, y)$, it is quite easy to see that \mathfrak{A} will again be diagonal (one may for instance rely on the fact that the operator \mathfrak{L} stays unchanged by a change of variable $(x, y) \rightarrow (x, -y)$). This remark immediately shows that the Haar based wavelet reduction cannot possibly lead to the ‘‘continuously’’ homogenized matrix when $Z_1 Z_2 \neq 0$. When $Z_1 = Z_2 = 0$ (which includes layered media) it is very easy to check that the formula (4.6) does agree with the ‘‘continuously’’ homogenized matrix.

Let us now turn our attention to the case when $A(x, y)$ is isotropic, *i.e.*, when $A^1(x, y) = A^2(x, y) = a(x, y)$. The function $a(x, y)$ is given by infinite periodic extension of the piecewise constant pattern

γ	δ
α	β

In this case the exact formula for the “continuously” homogenized matrix has recently been established (such a formula was, to the best of our knowledge, first conjectured in [16], but was only recently fully verified, as a special case of the results in [9]). The formula is

$$\mathfrak{A} = \begin{bmatrix} \sqrt{X\tilde{X}} & 0 \\ 0 & \sqrt{Y\tilde{Y}} \end{bmatrix},$$

with $X = X_1 = X_2 = h_x(m_y(a))$, $Y = Y_1 = Y_2 = h_y(m_x(a))$, $\tilde{X} = \tilde{X}_1 = \tilde{X}_2 = m_y(h_x(a))$, and $\tilde{Y} = \tilde{Y}_1 = \tilde{Y}_2 = m_x(h_y(a))$. In this case we have

$$\det(\mathfrak{A}) = \sqrt{X\tilde{X}Y\tilde{Y}} = XY - Z^2 = \det(H),$$

i.e., the coarse scale reduced matrix has the same determinant as the “continuously” homogenized matrix. We note that this determinant is independent of the location of the constants α, β, γ and δ in the pattern above; it only depends on the values of these constants, more precisely it is given by $P_3(\alpha, \beta, \gamma, \delta)/P_1(\alpha, \beta, \gamma, \delta)$, where P_n denotes the sum of all the $4!/(4-n)!n!$ products of n distinct constants. The traces are

$$\text{trace}(\mathfrak{A}) = \sqrt{X\tilde{X}} + \sqrt{Y\tilde{Y}}, \quad \text{and} \quad \text{trace}(H) = X \frac{X + \tilde{Y}}{X + Y} + Y \frac{\tilde{X} + Y}{X + Y} = X + Y - \frac{2Z^2}{X + Y},$$

respectively; these traces depend on the location of the constants and they are in general different. The special case of a two component “checkerboard” pattern, *i.e.*, the case when $a(x, y)$ is an infinite periodic extension of the pattern

β	α
α	β

was resolved much earlier (cf. [15] and [17]) by symmetry considerations and use of the celebrated Keller relation

$$\text{Hom}(kA/\det(A)) = k \text{Hom}(A)/\det(\text{Hom}(A))$$

between the homogenized matrix associated to the microstructure $kA(x, y)/\det(A(x, y))$ and that associated to $A(x, y)$ itself (k is any positive constant). It is quite easy to check that the wavelet based coarse scale reduction procedure does respect the Keller relation, indeed this follows from the fact that the coefficient transformation $(\alpha, \beta, \gamma, \delta) \rightarrow (\frac{1}{\alpha}, \frac{1}{\beta}, \frac{1}{\gamma}, \frac{1}{\delta})$ is associated with the $X - Y$ transformation

$(X, \tilde{X}, Y, \tilde{Y}) \rightarrow (\frac{1}{\tilde{Y}}, \frac{1}{Y}, \frac{1}{\tilde{X}}, \frac{1}{X})$. The Keller relation is also satisfied in the locally anisotropic case, *i.e.*, when $A^1 \neq A^2$. However, even here in the two component checkerboard case, the wavelet based coarse scale reduction does not reproduce the symmetry (isotropy) that is associated with the “continuous” homogenization procedure. Instead of $\mathfrak{A} = \sqrt{\alpha\beta} I_d$ (the “continuously” homogenized matrix) it leads to

$$\begin{aligned} H &= \begin{bmatrix} \frac{\alpha+\beta}{2} & 0 \\ 0 & \frac{\alpha+\beta}{2} \end{bmatrix} - \frac{1}{2} \left(\frac{\alpha+\beta}{2} - \frac{2\alpha\beta}{\alpha+\beta} \right) \begin{bmatrix} 1 & 1 \\ 1 & 1 \end{bmatrix} \\ &= \begin{bmatrix} \frac{\sqrt{2}}{2} & -\frac{\sqrt{2}}{2} \\ \frac{\sqrt{2}}{2} & \frac{\sqrt{2}}{2} \end{bmatrix} \begin{bmatrix} \frac{2\alpha\beta}{\alpha+\beta} & 0 \\ 0 & \frac{\alpha+\beta}{2} \end{bmatrix} \begin{bmatrix} \frac{\sqrt{2}}{2} & \frac{\sqrt{2}}{2} \\ -\frac{\sqrt{2}}{2} & \frac{\sqrt{2}}{2} \end{bmatrix}. \end{aligned}$$

This is exactly the “continuously” homogenized matrix associated with a layered medium of the two materials α and β , the layers being of equal thickness and orthogonal to the line $y = x$. Such a layering is in itself not an unreasonable discrete interpretation of the checkerboard pattern, however, it is interesting to note how this orientation is selected instead of the equally reasonable one, having layers parallel to the line $y = x$. In terms of invariants we have already seen that \mathfrak{A} and H have the same determinant, one may therefore be interested in knowing how far apart the values of the other invariant, the trace, really are. This question has a very precise answer in the two component checkerboard case, where

$$\text{trace}(\mathfrak{A}) = 2\sqrt{X^2 - Z^2}, \quad \text{and} \quad \text{trace}(H) = 2X - \frac{Z^2}{X} = \frac{2X^2 - Z^2}{X},$$

with $X = \frac{\alpha+\beta}{2}$, $Z = \frac{\alpha-\beta}{2}$. A simple calculation verifies that as a function Z , the expression $\frac{2X^2 - Z^2}{X}$ is the Padé approximation of numerator degree 3, denominator degree 1, $P_{3,1}(Z)$, of the expression $2\sqrt{X^2 - Z^2}$.

6 Multiwavelets: construction, differentiation and multiplication

A very natural approach to generalize the “homogenization” formulas obtained by means of the Haar basis, is to use higher order polynomials. Before proceeding along this direction we must briefly introduce the appropriate higher order polynomial wavelet setup. For simplicity we only study the case of piecewise linear functions, even though higher order polynomials might be relevant. Following Alpert [2] we use a Legendre (L^2 -orthogonal) basis. This has the advantage that it properly extends the Haar basis, and thus it makes direct comparisons easier and more relevant.

1. The new basis functions are :

- ϕ_0 – the first Legendre polynomial – given by $\phi_0 = \begin{cases} 1 & \text{if } 0 \leq x < 1 \\ 0 & \text{otherwise.} \end{cases}$
- ϕ_1 – the second Legendre polynomial – given by $\phi_1 = \begin{cases} \sqrt{3}(2x - 1) & \text{if } 0 \leq x < 1 \\ 0 & \text{otherwise.} \end{cases}$

2. The corresponding mother wavelets, *i.e.*, the two piecewise linear polynomials, needed to recover the scale functions at the next dyadic scale, are

The two parameters, θ and τ determine how a discontinuous function is averaged to obtain point values (at the right and the left endpoint respectively). For more details we refer the reader to [1].

Using the interscale relations and the above definition of the difference operators we may now represent the difference operators in a fashion that is consistent with the splitting $V_n = V_{n-1} \oplus W_{n-1}$. In doing so we interlace the variables, so that the coordinates corresponding to the four functions $\phi_0(x+k)$, $\phi_1(x+k)$, $\psi_0(x+k)$, and $\psi_1(x+k)$, for a fixed value of k , are consecutive. The structure of the difference operators stays as before, with the matrices R_{-1} , R_0 , and R_1 now given by

$$R_{-1} = \frac{\theta}{2} \begin{bmatrix} 1 & -\sqrt{3} & \sqrt{3} & -1 \\ \sqrt{3} & -3 & 3 & -\sqrt{3} \\ \sqrt{3} & -3 & 3 & -\sqrt{3} \\ 1 & -\sqrt{3} & \sqrt{3} & -1 \end{bmatrix}, \quad R_1 = \frac{\tau}{2} \begin{bmatrix} -1 & -\sqrt{3} & -\sqrt{3} & -1 \\ \sqrt{3} & 3 & 3 & \sqrt{3} \\ -\sqrt{3} & -3 & -3 & -\sqrt{3} \\ 1 & \sqrt{3} & \sqrt{3} & 1 \end{bmatrix},$$

$$R_0 = \frac{1}{2} \begin{bmatrix} \tau - \theta & \sqrt{3}(2 - \tau - \theta) & \sqrt{3}(\tau - \theta) & 6 - 5(\tau + \theta) \\ -\sqrt{3}(\theta + \tau) & 3(\tau - \theta) & 6 - 3(\tau + \theta) & \sqrt{3}(\tau - \theta) \\ \sqrt{3}(\tau - \theta) & -3(\tau + \theta) & 3(\tau - \theta) & 3\sqrt{3}(\tau + \theta) \\ -(\tau + \theta) & \sqrt{3}(\tau - \theta) & -\sqrt{3}(2 + \tau + \theta) & 9(\tau - \theta) \end{bmatrix}.$$

We notice that the top left 2×2 sub-matrices are simply the difference operator we started from, divided by 2. This is to be expected, and is entirely consistent with the change in scale between V_n and V_{n-1} .

Let $a(x)$ be a coarse scale periodic function which on the fine scale is simply given by $a(x) = \alpha\phi_0(2x) + \beta\phi_0(2x - 1)$. Multiplication with this function may, consistently with the splitting $V_n = V_{n-1} \oplus W_{n-1}$, be represented as a block diagonal matrix, where each block has the form

$$A_0 = \begin{bmatrix} \bar{a} & -\frac{\sqrt{3}}{2}\tilde{a} & 0 & \frac{1}{2}\tilde{a} \\ -\frac{\sqrt{3}}{2}\tilde{a} & \bar{a} & -\frac{1}{2}\tilde{a} & 0 \\ 0 & -\frac{1}{2}\tilde{a} & \bar{a} & -\frac{\sqrt{3}}{2}\tilde{a} \\ \frac{1}{2}\tilde{a} & 0 & -\frac{\sqrt{3}}{2}\tilde{a} & \bar{a} \end{bmatrix}$$

and the coefficients \bar{a} , and \tilde{a} are given by $\bar{a} = \frac{\alpha+\beta}{2}$ and $\tilde{a} = \frac{\alpha-\beta}{2}$. Here we lose one of the features of the multiwavelet approach, in that we only multiply with functions that are piecewise constant (and not piecewise linear).

7 Multiwavelet homogenization results

We now briefly describe the results we have obtained using the same reduction ideas as in sections 3 and 4 on the approximate second order operator assembled from the ingredients introduced above. We restrict ourselves to difference operators that can be understood as weighted quadrature rules, which amounts to taking $\tau = 1 - \theta$. We then have a family of difference operators depending on a single parameter, $D(\theta)$. In one dimension we reach a discrete approximation to the second order linear elliptic operator $\frac{d}{dx}(a(x)\frac{d}{dx}\cdot)$ by simply forming the matrix product $D(\theta_1)A_0D(\theta_2)$. We choose $\theta_2 = 1 - \theta_1$, to have a symmetric operator, $D(\theta)A_0D(1 - \theta)$, and we rearrange the variables so that the last element in each 4×4 block corresponds to the ‘‘flat’’ basis element ϕ_0 . This way our Gaussian elimination procedure leads to a reduced matrix for the coarse scale ‘‘flat’’ (Haar) variables. The operator considered in connection with the Haar basis, using a combination of a (complete) backward and a (complete) forward differentiation operator conceptually corresponds to the choice $\theta = 1$. It is essential for the Gaussian elimination process that θ be different from $\frac{1}{2}$, otherwise pivots will become zero; the same would be true in connection with the Haar basis if we had used a combination of a partial backward, and a partial forward differentiation operator. In one dimension, the coarse

scale reduction leads to the expected result: asymptotically we obtain the operator $D(\theta)HD(1-\theta)$ with H given by $H = \frac{\bar{a}^2 - \bar{\delta}^2}{\bar{a}} I_d = \frac{2\alpha\beta}{\alpha+\beta} I_d$. This result is independent of θ , and by continuity we may thus assign (the same) formula to $\theta = \frac{1}{2}$. The last remark is particularly relevant, since $\theta = \frac{1}{2}$ is a quite natural choice from an approximation point of view.

In the 2 dimensional case we decompose the fine scale discretization space as follows

$$\underbrace{V_x \times V_y}_V \oplus \underbrace{V_x \times W_y \oplus W_x \times V_y \oplus W_x \times W_y}_W.$$

This decomposition corresponds to the 16 basis vectors

$$\begin{array}{ll} V_x \times V_y & \phi_0(x)\phi_0(y), \phi_0(x)\phi_1(y), \phi_1(x)\phi_0(y), \phi_1(x)\phi_1(y) \\ V_x \times W_y & \phi_0(x)\psi_0(y), \phi_0(x)\psi_1(y), \phi_1(x)\psi_0(y), \phi_1(x)\psi_1(y) \\ W_x \times V_y & \psi_0(x)\phi_0(y), \psi_0(x)\phi_1(y), \psi_1(x)\phi_0(y), \psi_1(x)\phi_1(y) \\ W_x \times W_y & \psi_0(x)\psi_0(y), \psi_0(x)\psi_1(y), \psi_1(x)\psi_0(y), \psi_1(x)\psi_1(y). \end{array}$$

The coarse scale reduction is performed by generalization of the one dimensional procedure (in a fashion similar to what we did in section 4). The coefficient multiplication operator (and the homogenized matrix) is again conveniently expressed in terms of the ‘‘Haar’’ constants a_1, a_2, a_3 , and a_4 . Below we list the formulas for these constants (next to a picture of the corresponding period cell)

γ	δ
α	β

$$\begin{aligned} a_1 &= \frac{1}{4}(\alpha + \beta + \gamma + \delta). \\ a_2 &= \frac{1}{4}(\alpha + \beta - \gamma - \delta). \\ a_3 &= \frac{1}{4}(\alpha + \gamma - \beta - \delta). \\ a_4 &= \frac{1}{4}(\alpha + \delta - \beta - \gamma). \end{aligned}$$

The formula for the homogenized (coarse scale reduced) matrix now depends on the choice of θ ; this is contrary to the two dimensional Haar case, where we could also introduce partial backward and forward difference operators without affecting the formula for the coarse scale reduced matrix. For general θ the formula for the multiwavelet homogenized matrix is more complicated than previous formulas, and therefore difficult analytically to compare to these. One notable exception is the extremely natural choice $\theta = \frac{1}{2}$ where the result, as previously, may be expressed in terms of the three variables

$$\begin{aligned} X &= \frac{a_1^2 - a_3^2}{a_1} = h_x(m_y) \text{ harmonic average in } x \text{ of the average in } y \\ Y &= \frac{a_1^2 - a_3^2}{a_1} = h_y(m_x) \text{ harmonic average in } y \text{ of the average in } x \\ Z &= \frac{a_4 a_1 - a_2 a_3}{a_1} = \frac{\alpha\delta - \beta\gamma}{\alpha + \beta + \gamma + \delta} \text{ the normalized determinant.} \end{aligned}$$

In the case of the Haar basis

$$H_{Haar} = \begin{bmatrix} X & 0 \\ 0 & Y \end{bmatrix} - \frac{Z^2}{X+Y} \begin{bmatrix} 1 & 1 \\ 1 & 1 \end{bmatrix}.$$

For $H_{Legendre,1/2} = \lim_{\theta \rightarrow 1/2} H_{Legendre,\theta}$ we obtain the formula

$$H_{Legendre,1/2} = \begin{bmatrix} X - \frac{Z^2}{X+Y} & 0 \\ 0 & Y - \frac{Z^2}{X+Y} \end{bmatrix} - \frac{Z^4}{(X+Y)^3} \frac{1}{1 - 2\frac{Z^2}{(X+Y)^2}} \begin{bmatrix} 1 & 1 \\ 1 & 1 \end{bmatrix}.$$

The limiting formula is well defined, in spite of the fact that Gaussian elimination encounters zero pivots if attempted for $\theta = 1/2$. The result of “continuous” homogenization is

$$H = \begin{bmatrix} \sqrt{X\tilde{X}} & 0 \\ 0 & \sqrt{Y\tilde{Y}} \end{bmatrix}$$

with $\tilde{X} = m_y(h_x) = X - \frac{Z^2}{Y}$, the average in y of the harmonic average in x , and $\tilde{Y} = m_x(h_y) = Y - \frac{Z^2}{X}$, the average in x of the harmonic average in y . If we define the following map F of symmetric positive definite matrices to themselves

$$F \left(\begin{bmatrix} U & W \\ W & V \end{bmatrix} \right) = \begin{bmatrix} U & 0 \\ 0 & V \end{bmatrix} - \frac{W^2}{U+V} \begin{bmatrix} 1 & 1 \\ 1 & 1 \end{bmatrix},$$

then it is interesting to note that

$$H_{Haar} = F \left(\begin{bmatrix} X & Z \\ Z & Y \end{bmatrix} \right) \quad \text{while} \quad H_{Legendre,1/2} = F(H_{Haar}) = F^2 \left(\begin{bmatrix} X & Z \\ Z & Y \end{bmatrix} \right).$$

Since $\det(F(H)) = \det(H)$ we immediately conclude that $\det(H_{Legendre,1/2}) = \det(H_{Haar}) = \det(\mathfrak{A})$ (the determinant of the “continuously” homogenized matrix). The formula $H_{Legendre,1/2} = F(H_{Haar})$ holds even in the case when the original operator is anisotropic (but still diagonal). One may take that as an indication that the common expression $\det(H_{Legendre,1/2}) = \det(H_{Haar})$ is a good guess for the determinant of the “continuously” homogenized matrix. To compare the respective traces we introduce the variables

$$u = \frac{Z}{2(X+Y)} \in]-1, 1[\quad \text{and} \quad v = \frac{X-Y}{X+Y} \in]-1, 1[,$$

in terms of which we may now obtain the formulas

$$(\text{tr}(H_{Haar}))^2 - (\text{tr}(\mathfrak{A}))^2 = \left(\frac{X+Y}{2} \right)^2 \left[u^4 + \frac{4u^2v^2}{1-v^2} \right],$$

and

$$(\text{tr}(H_{Legendre,1/2}))^2 - (\text{tr}(\mathfrak{A}))^2 = \left(\frac{X+Y}{2} \right)^2 \left[\frac{u^8}{4(2-u^2)^2} + \frac{4u^2v^2}{1-v^2} \right].$$

We immediately conclude that the traces of H_{Haar} and $H_{Legendre,1/2}$ are both greater than the trace of the “continuously” homogenized matrix (thus the quadratic forms are both greater). The trace of $H_{Legendre,1/2}$ is the closer approximation to the trace of \mathfrak{A} . We now turn our attention to the two component checkerboard case

β	α
α	β

when $X = Y = \frac{\alpha+\beta}{2}$ and $Z = \frac{\alpha-\beta}{2}$. We calculate

$$\text{tr}(H_{\text{Legendre},1/2}) = 2X - \frac{Z^2}{X} - \frac{1}{2} \frac{Z^4}{X^2 \left(2X - \frac{Z^2}{X}\right)} = \frac{1}{2} \frac{8X^4 - 8X^2Z^2 + Z^4}{2X^3 - XZ^2},$$

which (as a function of Z) is easily seen to be the Padé approximant, $P_{5,3}(z)$, of numerator degree 5 and denominator degree 3 to the “continuously” homogenized trace $2\sqrt{X^2 - Z^2}$ (this compares to the Padé approximant of numerator degree 3, denominator degree 1, for H_{Har}). In this special case we furthermore calculate that

$$\lim_{n \rightarrow \infty} F^n \begin{bmatrix} X & Z \\ Z & X \end{bmatrix} = \begin{bmatrix} \sqrt{\alpha\beta} & 0 \\ 0 & \sqrt{\alpha\beta} \end{bmatrix},$$

the right hand side being the “continuously” homogenized matrix. A similar formula does not seem to hold in general.

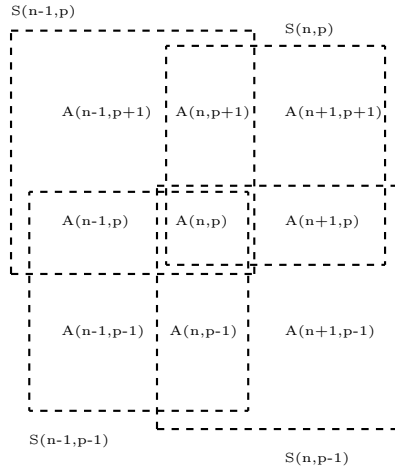
8 Computational results

The (coarse scale reduction) averaging formulas presented in sections 4 and 5 were derived under the assumption of periodicity of the coefficients. For simplicity we also restricted our discussion of these formulas to the case where the eigenvectors of the individual components were aligned with the coordinate axes. Numerically, however, we have carried out investigations in many cases where both of these assumptions are violated. As an example, consider the following elliptic operator

$$L = \frac{\partial}{\partial x} A^{xx}(x, y) \frac{\partial}{\partial x} + \frac{\partial}{\partial y} A^{yy}(x, y) \frac{\partial}{\partial y} + \frac{\partial}{\partial x} A^{xy}(x, y) \frac{\partial}{\partial y} + \frac{\partial}{\partial y} A^{xy}(x, y) \frac{\partial}{\partial x} \text{ on } [0, 1]^2$$

where the coefficients A^{xx} , A^{yy} and A^{xy} are constant on each one of 6400 (80×80) “pixels”, as displayed in Figure 8.1.

Due to the lack of periodicity there is not (even locally) a single representative 2×2 stencil on which our averaging formulas can be used. Each “pixel” (n, p) , to which corresponds 3 diffusion coefficients $A^{xx}(n, p)$, $A^{yy}(n, p)$ and $A^{xy}(n, p)$, belongs to four natural stencils, as shown in the picture below.



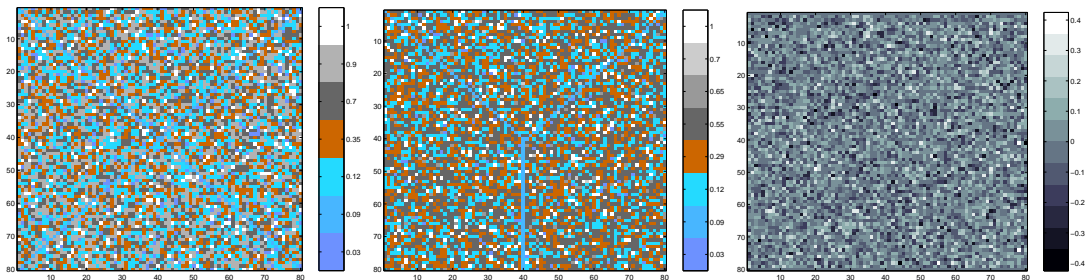


Figure 8.1: The diffusion coefficients A^{xx} , A^{yy} and A^{xy} .

The left image represents the A^{xx} coefficient, which takes 7 different values: 1 (307 times), 0.9 (1584), 0.7 (1272), 0.35 (1232), 0.12 (1576), 0.09 (160), 0.03 (269). Its mean is $m = 0.51$ and its standard deviation is $\sigma = 0.34$.

The center image represents the A^{yy} coefficient, which takes 8 different values: 1 (322 times), 0.7 (29), 0.65 (124), 0.55 (2498), 0.29 (1662), 0.12 (1528), 0.09 (120), 0.03 (117). For A^{yy} , $m = 0.39$ and $\sigma = 0.24$.

The right image displays the A^{xy} coefficient which, to ensure ellipticity, was constructed by the formula

$$A^{xy}(n, p) = \omega(n, p) \sqrt{A^{xx}(n, p)A^{yy}(n, p) - 10^{-4}} \quad ,$$

where $\omega(n, p)$ is a random number in $[-1, 1]$. For A^{xy} , $m = -0.0018$ and $\sigma = 0.11$.

For “pixels” with stencils that fall outside of the domain, the associated values are generated by periodic extension. To each “pixel” (n, p) we thus have four triplets of averaged coefficients, $H(S(n-1, p-1))$, $H(S(n-1, p))$, $H(S(n, p-1))$, and $H(S(n, p))$. We now use these four (triplets of) coefficients

$H(S(n-1, p))$	$H(S(n, p))$
$H(S(n-1, p-1))$	$H(S(n, p-1))$

as the new input 2×2 stencil for our averaging formulas. The corresponding averaged coefficients are associated to the “pixel” (n, p) . What has been described so far represents one step of averaging. We may iterate this procedure any number of times, for instance until the relative variation in the coefficients between two consecutive steps becomes smaller than 5% (which, in the present example, is true for all the averaging formulas after 9 steps). This iterated averaging method can be viewed as an analog of classic discrete diffusion schemes. In the case of a 2×2 periodic pattern the result (after one step) is a constant. In the case of periodic laminates parallel to one of the axes (but of arbitrary period) the iterated averaging asymptotically agrees with “continuous” homogenization. In such a situation, the conductivity matrices are diagonal at each step, and iterating the procedure corresponds to iteratively average arithmetically in one direction, and harmonically in the other. For the example we consider here we need averaging formulas that apply to conductivity matrices, that are not necessarily diagonal. Even if we had started out with an operator in diagonal form, this structure might not be preserved after one step of averaging, and so to perform any additional steps we would need such non-diagonal formulas. In the case of the Haar basis, the non-diagonal formulas may again be calculated explicitly (and our numerical results are based on these explicit formulas). Figure 8.2 shows the effect on the coefficient A^{xx} , of 9 explicit, Haar based averaging steps. For multiwavelets, however, the situation is slightly different. While it is in principle possible to derive explicit formulas

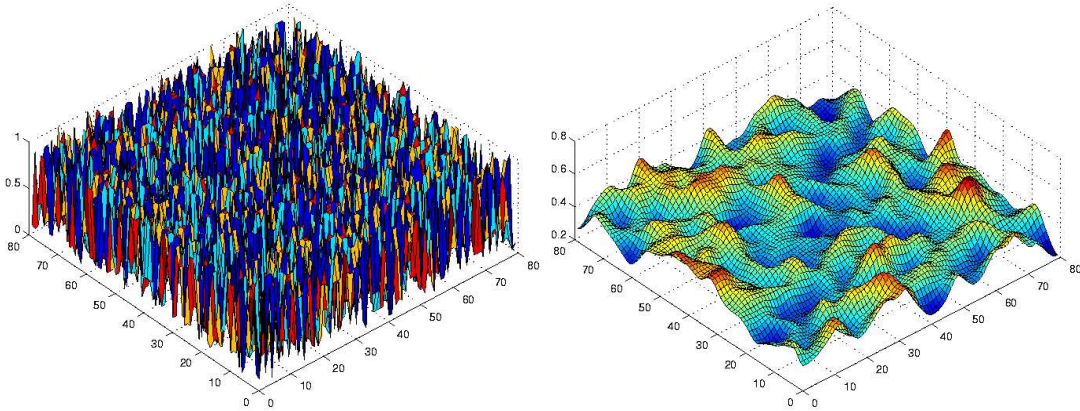


Figure 8.2: The original (left) and averaged (right) A^{xx} coefficient. The shown averaged coefficient is obtained using the explicit non-diagonal Haar formulas.

corresponding to the completely general non-diagonal case, the derivation of these appears to be beyond the scope of any of the standard symbolic algebra software packages, such as Maple or Fermat (a computational algebra program specialized in rational function manipulation). In place of an explicit formula we substitute an explicit procedure which arrives at the averaged coefficients by numerically performing a 16×16 Gaussian elimination independently at each of the 80×80 “pixels”. These Gaussian eliminations (that replace explicit formulas) were performed using Matlab routines. We note that this (local) approach is still far less costly than a full multiscale reduction procedure. We also note that it readily parallelizes. For further details about the programs used in the computations presented in this section we refer the reader to <http://www.math.rutgers.edu/~ycrc/WaveHom/>.

In order to evaluate the effectiveness of our averaging procedures (as far as solutions to the corresponding boundary value problems are concerned) we compute the eigenvalues in the range $[0, 106]$ for the problem

$$\begin{cases} L(u) = \lambda u \text{ in } \Omega = [0, 1]^2 \\ u = 0 \text{ on } \partial\Omega \end{cases} \quad (8.1)$$

Using P1 Finite Elements and the original (highly heterogeneous) coefficients, we calculate the approximate solution based on 5-6 different grids, starting with the same 80×80 rectangular grid used to define the coefficients, and successively refining it till we reach a 400×400 or 560×560 rectangular grid. The FE triangulations are obtained by subdividing each rectangle along its Northeast diagonal. Let us emphasize that the usage of a P1 finite element method to compute the solutions, for both the highly heterogeneous coefficients and their average counterpart was decided for simplicity, the only refinement parameter being in this case the grid size. One could certainly choose different resolution methods for both problems, the averaging procedure of the coefficients being completely independent of the resolution scheme adopted to compute solutions. In Figure 8.3 we compare eigenvalues computed in this fashion with the eigenvalues obtained from six different averaged coefficients (and use of the 80×80 discretization grid).

We make similar comparisons for certain average strains associated with the boundary value

problem

$$\begin{cases} L(u) = 0 \text{ in } \Omega = [0, 1]^2 \\ u(x, 0) = \sin(\pi x) \\ u(x, 1) = u(0, y) = u(1, y) = 0 \end{cases} \quad (8.2)$$

Here, we compute the average values of the gradient, $\int_{\Omega_i} \frac{\partial u}{\partial x}(s, t) ds dt$, on 16 sectors (or sub-domains) of size $\frac{1}{16}$: $[0, \frac{1}{4}] \times [0, \frac{1}{4}] \dots [\frac{3}{4}, 1] \times [\frac{3}{4}, 1]$. The comparisons arising from these computations are presented in Figure .8.4.

These computations clearly show that the wavelet based averaging formulas are effective, even in situations for which they were not designed – much more effective than the simplest combination of averages and harmonic averages. The wavelet based averaging formulas on the 80×80 grid give at least the same accuracy as a “brute force approach” based on 9 times as many degrees of freedom (the 240×240 grid). Iterated averaging produces a smoother coefficient, and fairly accurate numerical solutions may thus be obtained with relatively coarse grids (even coarser than the 80×80 used here). However, due to the additional smoothness of the coefficients, iterated averaging may, in cases without any apparent (periodic) structure, lead to solutions that are further from the “true” solutions than those obtained using a single step averaging. It is interesting to note that, for the eigenvalue computations, the additional numerical error one should encounter when using the single step averaging formulas has no negative effect as far as comparisons to the “true” (reference) values are concerned. The Haar based and the multiwavelet based averaging formulas appear equivalent for the eigenvalue computations. For the average strain computations we notice small differences – for instance if we consider the four “internal subdomains” numbered 6, 7, 10 and 11 (where boundary layer phenomena are minimal) then the multiwavelet based averaging gives slightly superior results at 7 and 10, and slightly inferior results at 6 and 11. There is no reason the multiwavelet based averaging formulas should lead to better results than the Haar based formulas, since, after all, we are using the same 80×80 grid for our finite element computations.

Acknowledgements

This research was partially supported by NSF grants DMS-0072556 and INT-0003788.

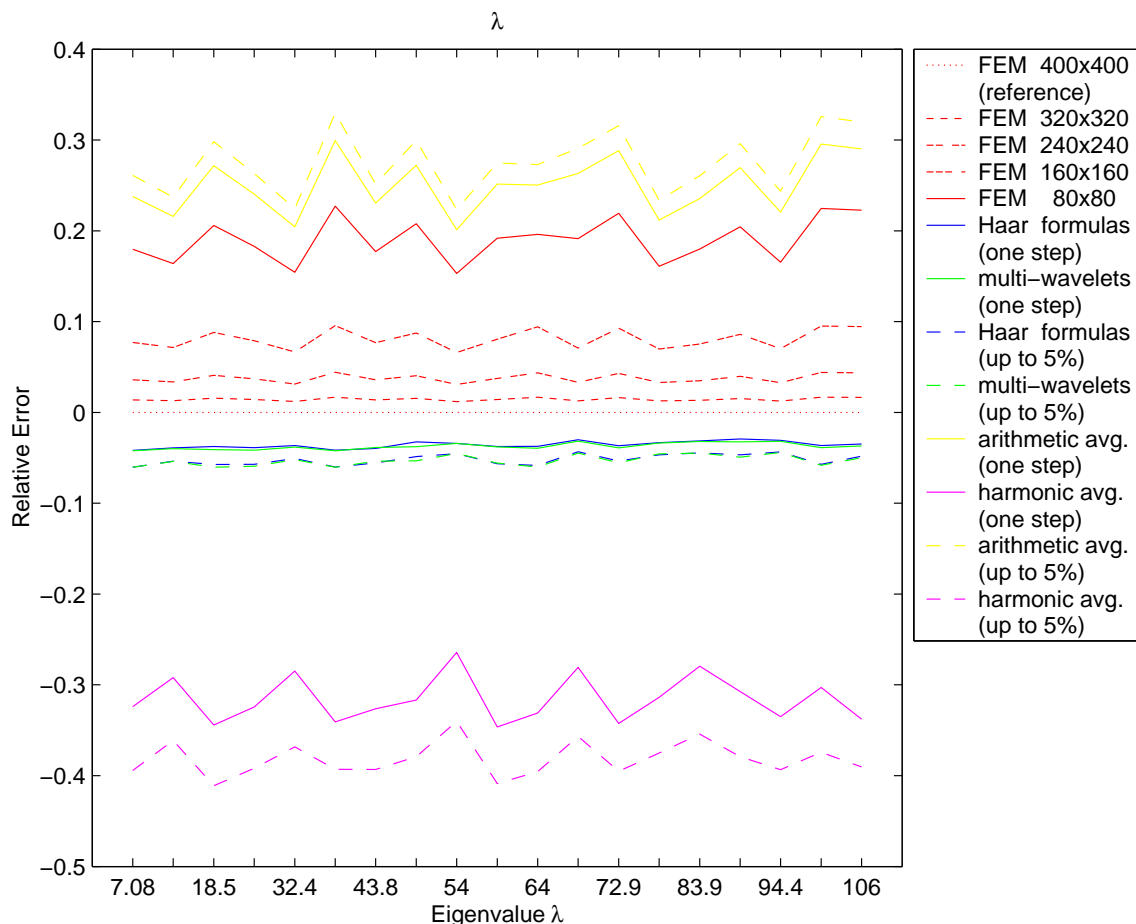


Figure 8.3: Finite element computation of the (first ≈ 17) eigenvalues of problem (8.1):

This figure displays the relative eigenvalue differences $\lambda - \lambda_{ref}/\lambda_{ref}$ (the “relative errors”) where, as λ_{ref} , we use the eigenvalues corresponding to a 400×400 rectangular grid, and the original, highly heterogeneous coefficients.

The “relative errors” in red correspond to eigenvalues obtained using the original coefficients, starting with the 80×80 discretization grid (solid) and going through successive refinements (dashed).

The “relative errors” in blue (resp. green) correspond to eigenvalues for the averaged coefficients obtained using the Haar basis (resp. the multiwavelet basis) and the 80×80 discretization grid.

The “relative errors” in yellow correspond to the eigenvalues where our averaging “formulas” have been replaced by plain arithmetic averages.

The “relative errors” in purple correspond to the eigenvalues where our averaging “formulas” have been replaced by harmonic averages as far as the diagonal entries are concerned, plain averages as far as the off diagonal entries are concerned.

Solid lines correspond to eigenvalues obtained using the coefficients coming from a single averaging step, whereas the dashed lines correspond to eigenvalues using the coefficients obtained after 9 averaging steps.

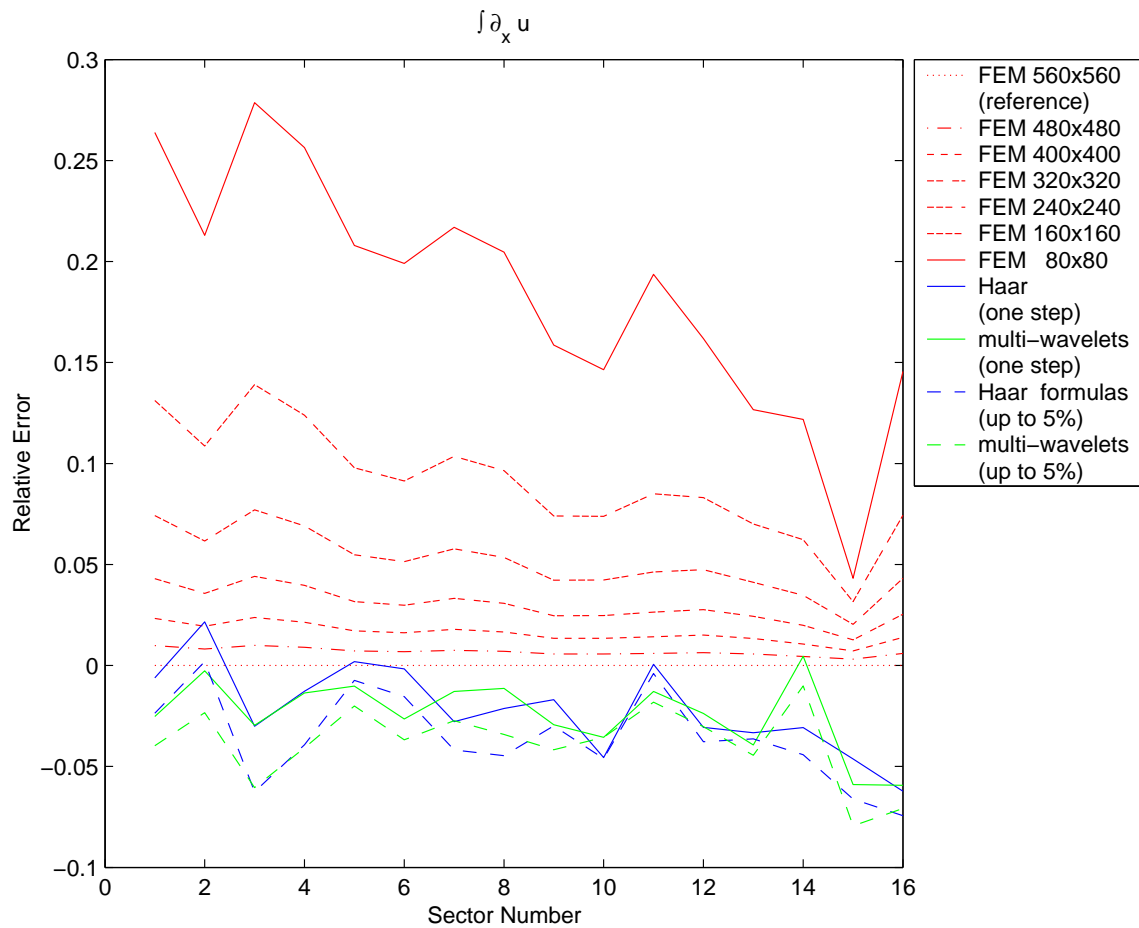


Figure 8.4: Finite element computation of 16 average gradients for the solution of problem (8.2):

This figure displays the “relative errors” in the 16 average gradients, where, as a reference we use the solution corresponding to the original, highly heterogeneous coefficients, and a 560×560 discretization grid. The abscissa represents the sector number, the ordering being from left to right and bottom to top

The “relative errors” in red correspond to the values obtained using the original coefficients, starting with the 80×80 grid (solid) and going through successive refinements (dashed).

The “relative errors” in blue (resp. green) correspond to computations performed with the averaged coefficients obtained using the Haar basis (resp. the multiwavelet basis) on the 80×80 discretization grid. Solid lines correspond to values obtained using the coefficients resulting from a single averaging step, whereas dashed lines correspond to values obtained using the coefficients based on 9 averaging steps.

References

- [1] B. Alpert, G. Beylkin, D. Gines, and L. Vozovoi. Adaptive solution of partial differential equations in multiwavelet bases. *J. Comput. Phys.*, 182(1):149–190, 2002.
- [2] B. K. Alpert. A class of bases in L^2 for the sparse representation of integral operators. *SIAM J. Math. Anal.*, 24(1):246–262, 1993.
- [3] U. Andersson, B. Engquist, G. Ledfelt, and O. Runborg. A contribution to wavelet-based subgrid modeling. *Appl. Comput. Harmon. Anal.*, 7(2):151–164, 1999.
- [4] T. Arbogast, S. E. Minko, and P. T. Keenan. An operator-based approach to upscaling the pressure equation. In V.N. Burganos et al., editor, *Computational Methods in Water Resources XII, Vol. 1: Computational Methods in Contamination and Remediation of Water Resources*, pages 405–412. Computational Mechanics Publications, 1998.
- [5] A. Bensoussan, J.-L. Lions, and G. Papanicolaou. *Asymptotic analysis for periodic structures*. North-Holland Publishing Co., Amsterdam, 1978.
- [6] G. Beylkin, R. Coifman, and V. Rokhlin. Fast wavelet transforms and numerical algorithms. I. *Comm. Pure Appl. Math.*, 44(2):141–183, 1991.
- [7] G. Beylkin and N. Coult. A multiresolution strategy for reduction of elliptic PDEs and eigenvalue problems. *Appl. Comput. Harmon. Anal.*, 5(2):129–155, 1998.
- [8] M. E. Brewster and G. Beylkin. A multiresolution strategy for numerical homogenization. *Appl. Comput. Harmon. Anal.*, 2(4):327–349, 1995.
- [9] R. V. Craster and Yu. V. Obnosov. Four-phase checkerboard composites. *SIAM J. Appl. Math.*, 61(6):1839–1856 (electronic), 2001.
- [10] M. Dorobantu and B. Engquist. Wavelet-based numerical homogenization. *SIAM J. Numer. Anal.*, 35(2):540–559, 1998.
- [11] B. Engquist and O. Runborg. Wavelet-based numerical homogenization with applications. In *Multiscale and multiresolution methods*, volume 20 of *Lect. Notes Comput. Sci. Eng.*, pages 97–148. Springer, Berlin, 2002.
- [12] A. C. Gilbert. A comparison of multiresolution and classical one-dimensional homogenization schemes. *Appl. Comput. Harmon. Anal.*, 5(1):1–35, 1998.
- [13] M. Griebel and S. Knapek. A multigrid-homogenization method. In R. Helmig, W. Jäger, W. Kinzelbach, P. Knabner, and G. Wittum, editors, *Modeling and Computation in Environmental Sciences*, volume 59 of *Notes on Numerical Fluid Mechanics*, pages 187–202, Braunschweig, 1997. Vieweg-Verlag.
- [14] T. Y. Hou and X. H. Wu. A multiscale finite element method for elliptic problems in composite materials and porous media. *J. Comput. Phys.*, 134:169–189, 1997.
- [15] J. B. Keller. A theorem on the conductivity of a composite medium. *J. Mathematical Phys.*, 5:548–549, 1964.
- [16] S. Mortola and S. Steffé. A two-dimensional homogenization problem. *Atti Accad. Naz. Lincei Rend. Cl. Sci. Fis. Mat. Natur. (8)*, 78(3):77–82, 1985.
- [17] J. Nevard and J. B. Keller. Reciprocal relations for effective conductivities of anisotropic media. *J. Math. Phys.*, 26(11):2761–2765, 1985.
- [18] Ph. Renard and G. de Marsily. Calculating equivalent permeability: a review. *Adv. Water Resour.*, 20(5-6):253–278, 1997.

Appendix

In this appendix, we provide the exact formulas for the coefficients appearing during the Gaussian elimination in section 4. As in section 4, the constants $c_{0,i}$, $c_{1,i}$, $c_{2,i}$, and $c_{3,i}$ denote the coefficients of the decomposition

$$L_{ii}^{(i)} = c_{0,i}I_d + c_{1,i}\Delta_{xx} + c_{2,i}\Delta_{yy} + c_{3,i}\Delta_{xy} + h^4R .$$

We also introduce the auxiliary constants $\alpha_1 = (a_1^2 + a_1^1)$, and $\alpha_2 = a_1^2a_1^1 + (a_1^1)^2 - (a_2^1)^2$.

$$\begin{aligned} c_{0,1} &= -16\alpha_1 < 0 \\ c_{1,1} &= -2(a_1^1 + a_3^1) \\ c_{2,1} &= -2(a_1^2 + a_2^2) \\ c_{3,1} &= 0 \\ \alpha_1 c_{0,2} &= -16\alpha_2 < 0 \\ -\frac{1}{2}(\alpha_1)^2 c_{1,2} &= a_1^1(a_1^2)^2 + 2a_1^2(a_1^1)^2 + (a_1^1)^3 + a_3^1(a_1^2)^2 + 2a_3^1a_1^2a_1^1 + a_3^1(a_1^1)^2 \\ &\quad - 2a_1^2(a_2^1)^2 - (a_2^1)^2a_1^1 - 2a_2^1a_1^2a_4^1 - 2a_2^1a_4^1a_1^1 + (a_2^1)^2a_3^1 \\ (\alpha_1)^2 c_{2,2} &= 2a_2^2a_1^2a_1^1 + 2a_2^2(a_1^1)^2 + (a_1^1)^3 + 3a_1^1(a_1^2)^2 + 2a_1^2(a_1^1)^2 - (a_2^2)^2a_1^1 \\ &\quad - (a_2^2)^2a_1^1 - 2a_1^2(a_2^1)^2 - 2(a_2^1)^2a_2^2 \\ c_{3,2} &= 0 \\ \alpha_2 c_{0,3} &= -16\left(a_1^1\left((a_1^2)^2 - (a_3^2)^2\right) + a_1^2\left((a_1^1)^2 - (a_2^1)^2\right)\right) < 0 \\ (\alpha_2)^2 c_{1,3} &= -4(a_2^1)^2(a_1^1)^2a_1^2 + 2a_2^1a_3^1a_4^1a_1^1 - (a_4^1)^2(a_1^1)^3 - 2(a_4^1)^2a_1^2(a_1^1)^2 - (a_4^1)^2a_1^1(a_1^2)^2 \\ &\quad - (a_3^1)^2a_1^2(a_1^1)^2 - (a_3^1)^2(a_1^1)^3 + 2(a_2^1)^2(a_3^2)^2a_1^1 - a_1^1(a_1^2)^2(a_2^1)^2 + 2(a_1^1)^3(a_1^2)^2 \\ &\quad + 3(a_1^1)^4a_1^2 + 2(a_1^1)^3a_3^1a_1^2 + 2(a_1^1)^2a_3^1(a_1^2)^2 - 2(a_2^1)^3a_4^1a_3^1 + (a_4^1)^2a_1^1(a_2^1)^2 \\ &\quad + (a_3^1)^2a_1^1(a_2^1)^2 - 2(a_2^1)^2(a_3^2)^2a_3^1 + a_1^2(a_4^1)^2(a_2^1)^2 + 2a_1^2(a_2^1)^3a_4^1 - 2(a_3^2)^2a_3^1(a_1^1)^2 \\ &\quad + 4(a_3^2)^2a_2^1a_4^1a_1^1 + 2a_2^1a_3^1a_4^1(a_1^1)^2 - 2a_2^1a_4^1(a_1^1)^2a_1^2 - 2a_2^1a_4^1a_1^1(a_1^2)^2 - 2(a_2^1)^2a_3^1a_1^2a_1^1 \\ &\quad + (a_1^1)^5 - 2(a_3^2)^2(a_1^1)^3 - 2(a_2^1)^2(a_1^1)^3 + (a_2^1)^4a_1^1 + a_1^2(a_2^1)^4 \\ -(\alpha_2)^2 c_{2,3} &= -4(a_2^1)^2(a_1^1)^2a_1^2 + 2a_2^1a_3^2a_1^1(a_2^1)^2 - (a_2^1)^2(a_3^2)^2a_1^2 + 3(a_2^1)^2(a_3^2)^2a_1^1 - 4a_1^1(a_1^2)^2(a_2^1)^2 \\ &\quad + 4(a_1^1)^3(a_1^2)^2 + 2(a_1^1)^4a_1^2 + 2(a_1^1)^2(a_1^2)^3 - (a_4^2)^2(a_2^1)^2a_1^1 - a_1^2(a_4^2)^2(a_2^1)^2 + (a_4^2)^2a_1^1(a_1^2)^2 \\ &\quad + 2(a_4^2)^2a_1^2(a_1^1)^2 - 3(a_3^2)^2(a_1^1)^3 - 4a_2^1a_1^2a_1^1(a_2^1)^2 - 2a_2^1a_3^2a_1^1(a_1^1)^2 + 4a_2^1(a_1^1)^3a_1^2 \\ &\quad + 2a_2^1(a_1^1)^2(a_1^2)^2 - 4a_2^1(a_2^1)^2(a_1^1)^2 - 2(a_3^2)^2a_1^2(a_1^1)^2 - 2a_4^2a_3^2(a_1^1)^3 + 2a_2^1(a_1^1)^4 + 2(a_2^1)^4(a_2^2) \\ &\quad + 2a_1^2(a_2^1)^4 + (a_2^2)^2(a_3^2)^2a_1^1 - 2a_2^1a_3^2a_4^2a_1^1 - 2a_2^1a_3^2a_4^2(a_1^1)^2 + (a_4^2)^2(a_1^1)^3 + 2a_2^1a_3^2a_4^2(a_2^1)^2 \\ \frac{1}{2}\alpha_2 c_{3,3} &= -a_2^1a_2^2a_3^2 - a_2^1a_3^1a_3^2 + a_4^1a_3^2a_1^1 - a_4^2a_2^1a_3^1 - a_2^2a_3^2a_4^1 + a_4^2a_2^1a_1^2 + a_4^1a_4^2a_1^2 + a_4^1a_4^2a_1^1 \end{aligned}$$